Journal of Statistical Physics, Vol. 77, Nos. 5/6, 1994

The Markov Property Method Applied to Ising Model Calculations

George A. Baker, Jr.[1]

Received December 31, 1993; final May 31, 1994

An efficient method of computation for models possessing the Markov property is set out. We apply this method to the two-dimensional Ising model and report exact computations for up to 10 by 10 models with periodic boundary conditions. We find that critical-point, finite-size rounding is quite large in the renormalized coupling constant, which is not divergent at the critical point, in contrast to the energy, which is also not divergent and has no rounding there. The difference is traced to the continuity of the energy and the discontinuity of the renormalized coupling constant at the critical point.

KEY WORDS: Markov property; Ising model; critical phenomena, parallel computational procedures.

1. INTRODUCTION AND SUMMARY

With the introduction of parallel computers, there is a strong motivation to reconsider the various methods of computation to see if the introduction of parallel processing ideas can be beneficial. One such idea is that of the Markov property.[3] A large class of problems possesses this property. Consider a region $\mathscr{R}$, interior to a domain $\mathscr{D}$ over which the problem is stated. Let the problem variables on the boundary $\partial\mathscr{R}$ of $\mathscr{R}$ be fixed, where $\partial\mathscr{R} \cap \mathscr{R} = \varnothing$. This statement is meant to include values, derivatives, etc., where appropriate. Then the problem is said to possess the Markov property if any expectation value of problem variables supported only in $\mathscr{R}$ is independent of all the problem variables supported in $\mathscr{D}\backslash(\mathscr{R} \cup \partial\mathscr{R})$, conditional on the problem variables in $\partial\mathscr{R}$. That is to say, if in the nearest-neighbor Ising model, we fix the boundary spins of an $n \times n$ square, the

[1] Theoretical Division, Los Alamos National Laboratory, University of California, Los Alamos, New Mexico 87545. gbj@griffin.lanl.gov.

822/77/5-6-1

expectation value of a spin in the interior of the square depends only on those fixed boundary spins, and not at all on anything that is outside the square. In this paper, we will investigate first how these ideas can be profitably applied to computation of the statistical mechanical properties of nearest-neighbor Ising-models on small, square regions of the plane-square lattice. In addition, we will study the implications for finite-size scaling of our results. We have a rather more complete set of data than has been previously available for such an investigation. Our principal conclusions are: One, the Markov property ideas are very effective for finite-size calculations [we have completed the exact computations for a 10×10 square (about 10^{30} states) on a workstation], and two, the "critical-point rounding" of finite-size scaling theory applies, not only to thermodynamic functions which diverge at the critical point, as is usually discussed, but also to functions which are finite at the critical point such as the renormalized coupling constant g, which turns out to be strongly "rounded." Nevertheless, the energy is not rounded, as was already known,[12] and may have lead some unwary not to be alert to this possibility.

In the second section, we describe the necessary formalism to decompose a problem into small blocks which can be summed over independently, and so computed in parallel. When there are only a finite number of types of small blocks, this computation can be done in advance, and the results saved for future use. We carry this formalism as far as the four-point correlation functions which are necessary to compute the second partial derivative of the magnetic susceptibility with respect to the magnetic field, and also far enough to compute the correlation length, the energy, and the specific heat.

In the third section, we show how this formalism can be utilized to compute progressively larger blocks by tabulation and relatively short computations. We show how these blocks can be simply combined to produce finite squares with periodic boundary conditions. Specifically we are working on the two-dimensional Ising model and we use diamonds for our blocks. It is straightforward to make bigger diamonds from smaller ones and also to compose squares with periodic boundary conditions out of the diamonds.

In the final section, we report and analyze our numerical results. We report the energy, the correlation length, the magnetic susceptibility, its second derivative with respect to the magnetic field, and the renormalized coupling constant for 2×2, 4×4, 6×6, 8×8, and 10×10 Ising model squares with periodic boundary conditions. We report the behavior of $\chi/\xi^{\gamma/\nu}$, $(\partial^2\chi/\partial H^2)/\chi^{(\gamma+2\Delta)/\gamma}$ and the renormalized coupling constant, and find strong, critical-point, finite-size rounding for all of these ratios, even though they are finite at the critical point. The rounded value for the renor-

malized coupling constant is seen to be an intermediate value between the thermodynamic values for temperatures above and below the critical temperature, as the critical temperature is a point of nonuniform approach for this quantity. *This effect is in sharp contrast to that for the quantities usually discussed.* In those cases the values, although rounded, still converge to the expected result! We also report on Binder's cumulant ratio.[6] Our results for it at the critical temperature agree with those of Burkhardt and Derrida[8] obtained by the transfer matrix method.

2. BLOCK DECOMPOSITION FORMALISM

In order to use this method, there are a number of straightforward rules for combining the results obtained by the summation over the interior of a block. They are fairly simple extensions of the one-dimensional results given in Baker.[3] I give them in this section. The first rule is that the entire finite section of a space lattice on which the model under consideration is defined should be divided into smaller blocks. The surfaces of division pass through the vertices only and not through any of the edges of the underlying lattice. It is not necessary although often convenient that all the blocks be identical. We will specifically be interested in the following quantities. The magnetization,

$$M = |\mathscr{L}|^{-1} \sum_{i \in \mathscr{L}} \langle \sigma_i \rangle \tag{2.1}$$

where $\mathscr{L}$ is the finite section of the space lattice over which the problem is defined, σ_i are the "spin variables" of the model, $|\mathscr{L}|$ is the number of vertices in $\mathscr{L}$, and $\langle \cdot \rangle$ denotes the expectation value with respect to the weight function,

$$[Z(K, H)]^{-1} \exp\left(K \sum_{i \in \mathscr{L}} \sum_{\delta \in \mathscr{D}} \sigma_i \sigma_{i+\delta} + H \sum_{i \in \mathscr{L}} \sigma_i \right) \prod_{i \in \mathscr{L}} [f(\sigma_i)\, d\sigma_i] \tag{2.2}$$

where $K = J/kT$, with J the exchange energy, k Boltzmann's constant, and T the absolute temperature, $H = mh/kT$, with m the magnetic moment and h the magnetic field, and $Z(K, H)$ is the partition function and is defined by the requirement that the weight function (2.2) be normalized. The single-spin distribution function is given by $f(\sigma)$. The set $\mathscr{D}$ is one-half the set of nearest-neighbor vectors on the space lattice. It is chosen so that every edge of the lattice is counted once and only once. I have deliberately chosen to consider the case with only nearest-neighbor interactions. If there are further-neighbor interactions, the boundary of the blocks is necessarily thickened, and although straightforward, the treatment of the block–block interactions becomes much more elaborate.

The next quantity of interest is the energy,

$$E = |\mathscr{L}|^{-1} \sum_{\mathbf{i} \in \mathscr{L}} \sum_{\delta \in \mathscr{D}} \langle \sigma_{\mathbf{i}} \sigma_{\mathbf{i}+\delta} \rangle \tag{2.3}$$

In addition we are concerned with several more thermodynamic quantities which require multiple sums over the lattice. Specifically we consider the specific heat at constant magnetic field C_H, the magnetic susceptibility $\chi(K)$, the second moment definition of the correlation length $\xi(K)$, and the second derivative with respect to magnetic field of the magnetic susceptibility. They are given by

$$C_H(K) = |\mathscr{L}|^{-1} \sum_{\mathbf{i} \in \mathscr{L}} \sum_{\delta \in \mathscr{D}} \sum_{\mathbf{j} \in \mathscr{L}} \sum_{\theta \in \mathscr{D}} (\langle \sigma_{\mathbf{i}} \sigma_{\mathbf{i}+\delta} \sigma_{\mathbf{j}} \sigma_{\mathbf{j}+\theta} \rangle - \langle \sigma_{\mathbf{i}} \sigma_{\mathbf{i}+\delta} \rangle \langle \sigma_{\mathbf{j}} \sigma_{\mathbf{j}+\theta} \rangle) \tag{2.4}$$

$$\chi(k) = |\mathscr{L}|^{-1} \sum_{\mathbf{i} \in \mathscr{L}} \sum_{\mathbf{j} \in \mathscr{L}} \langle \sigma_{\mathbf{i}} \sigma_{\mathbf{j}} \rangle \tag{2.5}$$

$$\xi^2(K) = |\mathscr{L}|^{-1} \left[\sum_{\mathbf{i} \in \mathscr{L}} \sum_{\mathbf{j} \in \mathscr{L}} |\mathbf{i}-\mathbf{j}|^2 \langle \sigma_{\mathbf{i}} \sigma_{\mathbf{j}} \rangle \right] \Big/ [2\, d\chi(K)] \tag{2.6}$$

$$\frac{\partial^2 \chi}{\partial H^2} = |\mathscr{L}|^{-1} \sum_{\mathbf{i} \in \mathscr{L}} \sum_{\mathbf{j} \in \mathscr{L}} \sum_{\mathbf{k} \in \mathscr{L}} \sum_{\mathbf{l} \in \mathscr{L}} \langle \sigma_{\mathbf{i}} \sigma_{\mathbf{j}} \sigma_{\mathbf{k}} \sigma_{\mathbf{l}} \rangle - 3\, |\mathscr{L}|\, [\chi(K)]^2 \tag{2.7}$$

where d is the spatial dimension.

It is now convenient to introduce the block spin sums,

$$S_\nu = \sum_{\mathbf{i} \in \mathscr{B}_\nu} w(\nu, \mathbf{i})\, \sigma_{\mathbf{i}} \tag{2.8}$$

where $\mathscr{B}_\nu$ is the portion of the space lattice which comprises block ν, and $w(\nu, \mathbf{i})$ is the fraction of site $\mathbf{i}$ in block ν and is subject to the constraint

$$\sum_\nu w(\nu, \mathbf{i}) = 1, \qquad \forall \mathbf{i} \tag{2.9}$$

It follows immediately from (2.9) that $w = 1$ for any interior spin. Normally, in, for example, two dimensions, $w = 1/2$ for a spin on an edge, and $w = 1/4$ or $3/4$ for an exterior or interior corner spin, respectively on the square lattice. One could also have $w = 1/6$ or $1/3$ or $2/3$ or $5/6$ for a corner spin on a triangular lattice. We will now divide the sites on the lattice into those sites which are interior to some block and the rest, which we will call boundary spins and which set we will denote by $\mathscr{B}$. It is necessary in this

decomposition that no interior spin of one block be a nearest neighbor on the lattice to an interior spin of any other block. By (2.8) and property (2.9), we can write

$$\sum_{i \in \mathscr{L}} \sigma_i = \sum_{\nu} S_\nu \tag{2.10}$$

If we next define $\langle \cdot \rangle_{\mathscr{C}_\nu}$ as the constrained expectation value with respect to (2.2) within the νth block, with all the boundary spins fixed, and further define $\langle \cdot \rangle_{\mathscr{B}}$ to be the expectation with respect to the boundary spins, then we can write

$$M = |\mathscr{L}|^{-1} \left\langle \sum_{\nu} \left[\langle S_\nu \rangle_{\mathscr{C}_\nu} \prod_{\substack{\mu \\ \mu \neq \nu}} \langle 1 \rangle_{\mathscr{C}_\mu} \right] \right\rangle$$

$$= |\mathscr{L}|^{-1} \left\langle \left(\sum_{\nu} \frac{\langle S_\nu \rangle_{\mathscr{C}_\nu}}{\langle 1 \rangle_{\mathscr{C}_\nu}} \right) \prod_{\mu} \langle 1 \rangle_{\mathscr{C}_\mu} \right\rangle_{\mathscr{B}} \tag{2.11}$$

We observe that (2.11) has the form of a new quantity,

$$[S_\nu] \equiv \frac{\langle S_\nu \rangle_{\mathscr{C}_\nu}}{\langle 1 \rangle_{\mathscr{C}_\nu}} \tag{2.12}$$

which depends only on the boundary spins of $\mathscr{B}_\nu$, which set we denote as $\partial \mathscr{B}_\nu$, whose expectation value we are taking, with respect to all the boundary spins, $\mathscr{B} = \bigcup_\nu \partial \mathscr{B}_\nu$, by the use of an additional weighting factor,

$$\prod_{\mu} \langle 1 \rangle_{\mathscr{C}_\mu} \tag{2.13}$$

as displayed by (2.11).

It is instructive to go through in some detail the reduction of the susceptibility (2.5) to block form. By (2.10) we can write it as

$$\chi(K) = |\mathscr{L}|^{-1} \left\langle \sum_{\nu} \sum_{\mu} S_\nu S_\mu \right\rangle$$

which by the Markov property

$$= |\mathscr{L}|^{-1} \left\langle \sum_{\nu} (\langle S_\nu^2 \rangle_{\mathscr{C}_\nu} - \langle S_\nu \rangle_{\mathscr{C}_\nu}^2) + \sum_{\nu} \sum_{\mu} \langle S_\nu \rangle_{\mathscr{C}_\nu} \langle S_\mu \rangle_{\mathscr{C}_\mu} \right\rangle_{\mathscr{B}}$$

$$= |\mathscr{L}|^{-1} \left\langle \left\{ \sum_{\nu} ([S_\nu^2] - [S_\nu]^2) + \sum_{\nu} \sum_{\mu} [S_\nu][S_\mu] \right\} \prod_{\lambda} \langle 1 \rangle_{\mathscr{C}_\lambda} \right\rangle_{\mathscr{B}}$$

$$= |\mathscr{L}|^{-1} \left\langle (T_2 - T_3 + T_1^2) \prod_{\lambda} \langle 1 \rangle_{\mathscr{C}_\lambda} \right\rangle_{\mathscr{B}} \tag{2.14}$$

in the notation of (2.12) and where we define

$$T_1 = \sum_\nu [S_\nu], \qquad T_2 = \sum_\nu [S_\nu^2], \qquad T_3 = \sum_\nu [S_\nu]^2 \tag{2.15a}$$

In order to compute the second partial of the susceptibility in block decomposed form we will need the further quantities

$$T_4 = \sum_\nu [S_\nu^3], \qquad T_5 = \sum_\nu [S_\nu][S_\nu^2], \qquad T_6 = \sum_\nu [S_\nu]^3$$

$$T_7 = \sum_\nu [S_\nu^4], \qquad T_8 = \sum_\nu [S_\nu][S_\nu^3], \qquad T_9 = \sum_\nu [S_\nu^2][S_\nu]^2 \tag{2.15b}$$

$$T_{10} = \sum_\nu [S_\nu^2]^2, \qquad T_{11} = \sum_\nu [S_\nu]^4$$

With this notation we can directly express the intermediate quantities

$$\mathscr{T}_1 = \sum_{\mathbf{i}} \langle \sigma_{\mathbf{i}} \rangle = \left\langle T_1 \prod_\lambda \langle 1 \rangle_{\mathscr{C}_\lambda} \right\rangle_{\mathscr{B}}$$

$$\mathscr{T}_2 = \sum_{\mathbf{i}} \sum_{\mathbf{j}} \langle \sigma_{\mathbf{i}} \sigma_{\mathbf{j}} \rangle = \left\langle (T_2 - T_3 + T_1^2) \prod_\lambda \langle 1 \rangle_{\mathscr{C}_\lambda} \right\rangle_{\mathscr{B}}$$

$$\mathscr{T}_3 = \sum_{\mathbf{i}} \sum_{\mathbf{j}} \sum_{\mathbf{k}} \langle \sigma_{\mathbf{i}} \sigma_{\mathbf{j}} \sigma_{\mathbf{k}} \rangle = \left\langle (T_1^3 - 3T_1 T_3 + 2T_6 + 3T_1 T_2 - 3T_5 + T_4) \prod_\lambda \langle 1 \rangle_{\mathscr{C}_\lambda} \right\rangle_{\mathscr{B}} \tag{2.16}$$

$$\mathscr{T}_4 = \sum_{\mathbf{i}} \sum_{\mathbf{j}} \sum_{\mathbf{k}} \sum_{\mathbf{l}} \langle \sigma_{\mathbf{i}} \sigma_{\mathbf{j}} \sigma_{\mathbf{k}} \sigma_{\mathbf{l}} \rangle = \left\langle (T_1^4 - 6T_1^2 T_3 + 6T_1^2 T_2 - 6T_2 T_3 + 8T_1 T_6 - 12T_1 T_5 + 4T_1 T_4 + 3T_2^2 + 3T_3^2 - 6T_{11} + 12T_9 - 3T_{10} - 4T_8 + T_7) \prod_\lambda \langle 1 \rangle_{\mathscr{C}_\lambda} \right\rangle_{\mathscr{B}}$$

From these intermediate quantities, we can directly express the block decomposition formulas

$$\begin{aligned} M(K) &= \mathscr{T}_1/|\mathscr{L}| \\ \chi(K) &= \mathscr{T}_2/|\mathscr{L}| \\ \partial^2\chi(K)/\partial H^2 &= \mathscr{T}_4/|\mathscr{L}| - 3\,|\mathscr{L}|\,\{\chi(K)\}^2 \end{aligned} \tag{2.17}$$

The method of derivation of (2.16) is most simply expressed as follows. Consider, for example, the work for $\mathscr{T}_3$. The need is to find which parts are evaluated internal to a block and which parts are evaluated in separate blocks. We may rewrite $\mathscr{T}_3$ as

$$\begin{aligned} \mathscr{T}_3 = \Big\langle \sum_{\nu_1}\sum_{\nu_2}\sum_{\nu_2} &(1-\delta_{12}+\delta_{12})(1-\delta_{23}+\delta_{23}) \\ &\times(1-\delta_{13}+\delta_{13})[S_{\nu_1}S_{\nu_2}S_{\nu_3}]\prod_{\lambda}\langle 1\rangle_{\mathscr{C}_\lambda}\Big\rangle_{\mathscr{B}} \end{aligned} \tag{2.18}$$

where we have extended the bracket notation as

$$\Big[\prod_{j\in\mathscr{J}} S_j\Big] \equiv \frac{\prod_{j\in\mathscr{J}}\langle S_j\rangle_{\mathscr{C}_j}}{\prod_{j\in\mathscr{J}}\langle 1\rangle_{\mathscr{C}_j}} \tag{2.19}$$

and $\delta_{ij}=1$ if $\nu_i=\nu_j$ and $\delta_{ij}=0$ otherwise. The notation in (2.19) is meant to imply that if there is a repeat among the elements of $\mathscr{J}$, then the corresponding S_j appears as a power equal to the multiplicity m in the numerator $\langle S_j^m\rangle_{\mathscr{C}_j}$ and the products on the right-hand side are only over distinct elements. We next expand (2.18) as

$$\begin{aligned} \mathscr{T}_3 = \Big\langle \Big\{ &\sum_{\nu_1}\sum_{\nu_2}\sum_{\nu_2}(1-\delta_{12})(1-\delta_{23})(1-\delta_{13})[S_{\nu_1}][S_{\nu_2}][S_{\nu_3}] \\ &+3(/)\sum_{\nu_2}\sum_{\nu_2}(1-\delta_{23})[S_{\nu_2}^2][S_{\nu_3}] \\ &+(\Delta)\sum_{\nu_3}[S_{\nu_3}^3]\Big\}\prod_{\lambda}\langle 1\rangle_{\mathscr{C}_\lambda}\Big\rangle_{\mathscr{B}} \end{aligned} \tag{2.20}$$

where use has been made of the property $(1-\delta)^2=(1-\delta)$. There is a combinatorial interpretation of the coefficients. We have expanded in terms of the "$+\delta$" terms. They have the property of making the ν's agree and hence can be thought of as bonds (of infinite strength) between the vertices labeled by the values of ν. Since $\nu_1=\nu_2$ and $\nu_2=\nu_3$ implies $\nu_1=\nu_3$, these relations turn out to imply that the coefficients are the strong embeddings

of the linear graph shown in the little picture in parentheses on the complete three-graph (triangle). This remark is not such an improvement over straightforward calculation here, but is fairly helpful for $\mathscr{T}_4$. By a "strong embedding" is meant one for which the nearest neighbors on the underlying graph must also be nearest neighbors on the (unlabeled) embedded graph.[16] If this restriction does not apply, then we say we have a "weak embedding." If we now expand the $(1-\delta)$ factors in (2.20) and collect the terms, we obtain directly the results of (2.16). Note is made that the coefficients that we obtain for this expansion are the weak embedding coefficients. The details of the computation for $\mathscr{T}_4$ are given by Baker,[3] as his one-dimensional special case has no effect on this portion of the computation.

The block decomposition of the energy is quite straightforward. By our rules, every edge lies in a unique block. If we define an edge e_j by the two vertices $\mathbf{j}_1, \mathbf{j}_2$ which lie at its ends, then with the notation

$$E_\nu = \sum_{e_j \in B_\nu} \sigma_{\mathbf{j}_1} \sigma_{\mathbf{j}_2} \tag{2.21}$$

we easily get

$$E = |\mathscr{L}|^{-1} \left\langle \mathscr{E}_1 \prod_\lambda \langle 1 \rangle_{\mathscr{C}_\lambda} \right\rangle_{\mathscr{B}} \tag{2.22}$$

where

$$\mathscr{E}_1 = \sum_\nu [E_\nu], \qquad \mathscr{E}_2 = \sum_\nu [E_\nu^2], \qquad \mathscr{E}_3 = \sum_\nu [E_\nu]^2 \tag{2.23}$$

The results for the specific heat are simply given by the same methods as

$$C_H = |\mathscr{L}|^{-1} \left\langle (\mathscr{E}_2 - \mathscr{E}_3) \prod_\lambda \langle 1 \rangle_{\mathscr{C}_\lambda} \right\rangle_{\mathscr{B}} \tag{2.24}$$

The last quantity of interest is the correlation length ξ. We will not use (2.6) directly, since the factor $|\mathbf{i}-\mathbf{j}|^2$ can get quiet large. While it is true that the coefficient of this factor decays exponentially, if we wish to apply this method later to Monte Carlo estimation, then this feature causes unduly long runs. (We will not discuss Monte Carlo methods in this paper, but intend to do so in subsequent work.) Instead we will derive it from the momentum-dependent susceptibility.[10] We extend (2.5) to be

$$\begin{aligned} \chi(|\mathscr{L}|, \mathbf{q}, K) &= |\mathscr{L}|^{-1} \sum_{\mathbf{i} \in \mathscr{L}} \sum_{\mathbf{j} \in \mathscr{L}} \exp[i\mathbf{q} \cdot (\mathbf{i}-\mathbf{j})] \langle \sigma_{\mathbf{i}} \sigma_{\mathbf{j}} \rangle \\ &= \sum_\nu \sum_\mu \exp[i\mathbf{q} \cdot (\mathbf{R}_\nu - \mathbf{R}_\mu)] \langle S_\nu(\mathbf{q})\, S_\mu^*(\mathbf{q}) \rangle \end{aligned} \tag{2.25}$$

where $\mathbf{R}_\nu$ is the origin of block $\mathscr{B}_\nu$, the asterisk denotes complex conjugate, and

$$S_\nu(\mathbf{q}) = \sum_{\mathbf{j} \in \mathscr{B}_\nu} w(\nu, \mathbf{j}) \exp[i\mathbf{q} \cdot (\mathbf{j} - \mathbf{R}_\nu)]\, \sigma_{\mathbf{j}} \tag{2.26}$$

If we extend in a similar manner the definition (2.15) to give

$$T_1(\mathbf{q}) = \sum_\nu [S_\nu(\mathbf{q})], \qquad T_2(\mathbf{q}) = \sum_\nu [|S_\nu(\mathbf{q})|^2], \qquad T_3(\mathbf{q}) = \sum_\nu |[S_\nu(\mathbf{q})]|^2 \tag{2.27}$$

then we get

$$\chi(|\mathscr{L}|, \mathbf{q}, K) = |\mathscr{L}|^{-1} \left\langle (T_2(\mathbf{q}) - T_3(\mathbf{q}) + |T_1(\mathbf{q})|^2) \prod_\lambda \langle 1 \rangle_{\mathscr{C}_\lambda} \right\rangle_{\mathscr{B}} \tag{2.28}$$

which reduces to (2.16)–(2.17) when $\mathbf{q} = 0$. To obtain $\xi(K)$ from $\chi(|\mathscr{L}|, \mathbf{q}, K)$ we first note[10] that

$$\xi^2(K) = \frac{1}{4 \sum_{\tau=1}^{d} \sin^2(\frac{1}{2}\mathbf{q} \cdot e_\tau)} \left(1 - \frac{\chi(|\mathscr{L}|, \mathbf{q}, K)}{\chi(|\mathscr{L}|, \mathbf{0}, K)}\right) + O(|\mathbf{q}|^2) \tag{2.29}$$

to the given order, where e_τ are the unit vectors in each of the lattice directions. This formula is exact for the Gaussian model on the hyper-simple-cubic lattice family. For a finite lattice section, of course the $\mathbf{q}$ are a discrete set of vectors; however, for a large lattice section, there will be many of them which are small enough for us to be able to use this result effectively. For the one-dimensional Ising model, Baker[3] has shown that

$$4 \sum_{\tau=1}^{d} \sin^2\left(\frac{1}{2}\mathbf{q} \cdot e_\tau\right) \left(1 - \frac{\chi(|\mathscr{L}|, \mathbf{q}, K)}{\chi(|\mathscr{L}|, \mathbf{0}, K)}\right)^{-1} = \xi^{-2} + 4 \sum_{\tau=1}^{d} \sin^2\left(\frac{1}{2}\mathbf{q} \cdot e_\tau\right) \tag{2.30}$$

These remarks suggest that a good procedure to determine ξ is to select a method which assumes the form (2.30), at least for small $|\mathbf{q}|$.

3. BLOCK COMPOSITION

One can start with the direct computation of small blocks and use the formalism of the previous section to combine them to form larger blocks in a much more efficient manner than by the direct computation of the larger blocks. This result is a consequence of the Markov property. I will

illustrate the method in two dimensions. It appears that the most efficient way to break up the plane square lattice is to divide it into diamonds. The simplest such diamond is illustrated in Fig. 1, and has two vertices on each side. The weight function (unnormalized) and the block spin are

$$\exp(K(\sigma_1+\sigma_2+\sigma_3+\sigma_4)\,\sigma_5), \qquad S=\tfrac{1}{4}(\sigma_1+\sigma_2+\sigma_3+\sigma_4)+\sigma_5$$
$$E=(\sigma_1+\sigma_2+\sigma_3+\sigma_4)\,\sigma_5 \tag{3.1}$$

where σ_5 is the single interior spin and the rest are boundary spins. For the Ising model case, where the spin states are just $\sigma=\pm 1$, we can compute

$$\begin{aligned}
\langle 1\rangle_{\mathscr{G}} &= 2\cosh(K(\sigma_1+\sigma_2+\sigma_3+\sigma_4))\\
[S] &= \tfrac{1}{4}(\sigma_1+\sigma_2+\sigma_3+\sigma_4)+\tanh(K(\sigma_1+\sigma_2+\sigma_3+\sigma_4))\\
[S^2] &= \tfrac{1}{16}(\sigma_1+\sigma_2+\sigma_3+\sigma_4)^2\\
&\quad +\tfrac{1}{2}(\sigma_1+\sigma_2+\sigma_3+\sigma_4)\tanh(K(\sigma_1+\sigma_2+\sigma_3+\sigma_4))+1\\
&\quad \text{etc.}
\end{aligned} \tag{3.2}$$

where the necessary unlisted quantities are $[S^3]$, $[S^4]$, $[S(\mathbf{q})]$, $[|S(\mathbf{q})|^2]$, $[E]$, and $[E^2]$. They can also be computed in a straightforward manner, and tabulated numerically as a function of the 16 possible boundary conditions for fixed K. The next simplest diamond has 3 vertices on each side and is illustrated in Fig. 2. There are 5 interior vertices and 8 boundary ones. The required computation is a sum over 32 states for each of the 256 possible sets of boundary conditions. Of course, not all need to be computed, because the model has spin-reversal symmetry, and the diamond has a rotation and a reflection symmetry. In any event, this computation is very quickly done on even on a personal computer.

With these basic blocks (although the direct computation of the 3-diamond was in fact unnecessary) we can construct larger diamonds. For example, the four vertices per edge diamond can be built up of five

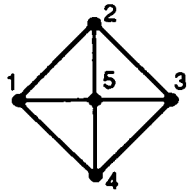

Fig. 1. The smallest or 2-diamond embedded on the plane-square lattice. Vertices 1–4 are boundary vertices and vertex 5 is interior.

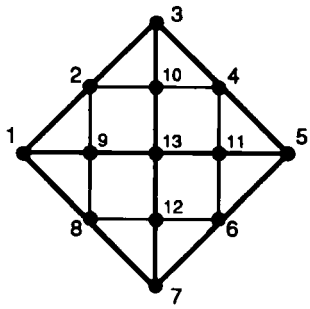

Fig. 2. The 3-diamond. Vertices 1–8 are boundary vertices and vertices 9–13 are interior.

2-diamonds and one 3-diamond as illustrated in Fig. 3. There are now 12 boundary spins and 3 internal spins which must be summed over to compete the calculation. That is a sum over 8 states for each of the 4096 possible boundary conditions.

We have found it quite possible to compute the tables for the 5-diamond and the 6-diamond. They were divided as shown in Fig. 4. There are four 3-diamonds in the 5-diamond, with 16 boundary spins over 65,536 possible boundary conditions and 5 internal spins or 32 states to sum over. It was convenient to introduce the 3×4 diamonds as shown in Fig. 4 as well to compute the 6-diamond. It is broken up into one 3-diamond and two 2-diamonds and so has 10 boundary spins or 1024 possible boundary conditions, but just one internal spin and so just 2 states to sum over. The 6-diamond is broken up into one 4-diamond, two 3×4

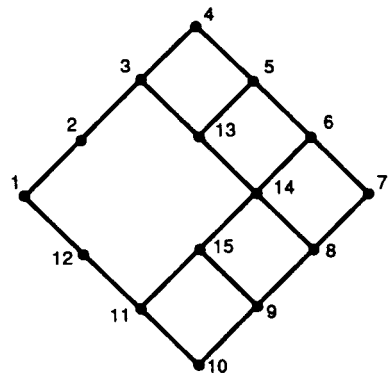

Fig. 3. The 4-diamond as decomposed into smaller diamonds. Vertices 1–12 are boundary vertices and vertices 13–15 are the interior vertices which remain to be summed over.

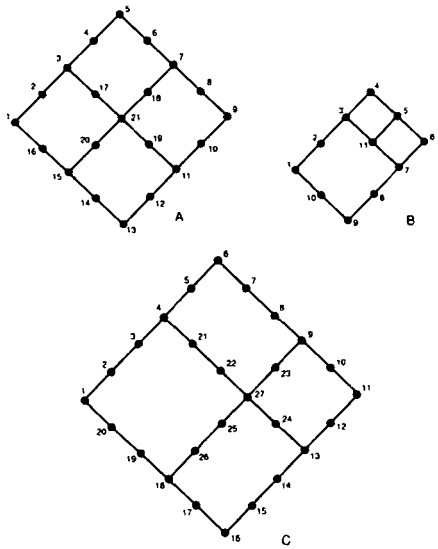

Fig. 4. (A) The 5-diamond as decomposed into smaller diamonds. Vertices 1–16 are boundary vertices and vertices 17–21 are the interior vertices which remain to be summed over. (B) The 3×4 diamond as decomposed into smaller diamonds. Vertices 1–10 are boundary vertices and vertex 11 is the interior vertex which remains to be summed over. (C) The 6-diamond decomposed into smaller diamonds. Vertices 1–20 are the boundary vertices and vertices 21–27 are the interior vertices which remain to be summed over.

diamonds, and one 3-diamond. There are 20 boundary spins or 1,048,576 possible boundary conditions and 7 internal spins or 128 states to sum over. The result is equivalent to a sum over the 41 internal spins or 2.2×10^{12} states for each of the 1.0×10^{6} possible boundary conditions. Attention must be paid to the orientation of the 3×4 diamond in

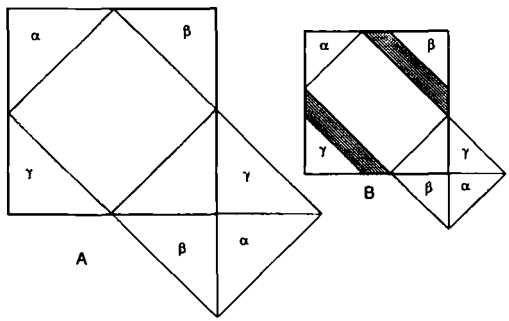

Fig. 5. The construction for the reorganization of two diamonds into a square whose edge is equal the the tip-to-tip width of the diamonds. (A) For squares whose edge length is even; (B) for odd squares. The trapezoidal bridges are the shaded areas.

computations involving $S(\mathbf{q})$. There may be a storage problem for the 6-diamond tables on some computers.

When periodic boundary conditions are used, it is possible to combine two diamonds of the same size to form a square. This construction will be the basis of the numerical results for square systems with periodic boundary conditions which are given in the next section. The construction is illustrated in Fig. 5A for squares whose edge length is even. The lower diamond is divided as shown and the pieces are shifted by the system periodicity so that the two triangles labeled with the same letter coincide. In the final sum over the boundary spins the corresponding boundary spins on the two triangles are set equal to each other. For squares whose edge length is odd, the construction is shown in Fig. 5B. Here we use an $(n+1)\times(n+2)$ rectangle, an $(n+1)$-diamond, and two trapezoidal bridges of unit thickness and edges $(n+1)$ and $(n+2)$ to form a $(2n+1)\times(2n+1)$ square. These bridges have no internal spin sums to be done.

4. EXACT CALCULATIONS FOR THE PLANE-SQUARE ISING MODEL

A great deal has been written about finite-size scaling theory. See for example, Barber,[4] Cardy,[9] and Privmann.[14] In its most elementary form, it is very compelling. That is to say, in models such as the Ising model for which we know that, except at the critical point, the spin–spin correlation functions decay strongly with distance, we expect validity of the following simple idea: If the ratio of the correlation length to the system size ξ/L is sufficiently small, then the difference between the estimates of extensive properties estimated from a finite-sized system of side L and those estimated from an infinite system can be made as small as one pleases by choosing L large enough. Since one never has an infinite system, a series of computations for progressively larger systems is commonly made for a set of different values of ξ/L and these results are then extrapolated to infinite system size. The results of the extrapolation to infinite system size for the different values of ξ/L are then extrapolated to give the result for the value $\xi/L=0$. Beyond this simple idea are deeper ideas which can be introduced as follows: Since the correlation length $\xi(K)$ in the infinite system is a monotonic (at least for the two-dimensional Ising model and numerically much more generally) function of K which runs from 0 to ∞ as K runs from zero to K_c, there is manifestly a function $\Phi_L(x)$ such that

$$\xi_L(K)/L=\Phi_L(\xi(K)/L) \tag{4.1}$$

The theory further shows, from various hypotheses, that there exists the limit

$$\Phi_\xi(x) = \lim_{L \to \infty} \Phi_L(x), \qquad \forall 0 \leqslant x \leqslant \infty \tag{4.2}$$

as a smooth function. For x small, one must have

$$\lim_{x \to 0} \Phi_\xi(x)/x = 1 \tag{4.3}$$

as all the $\xi_L^2(K) = K + O(K^2)$. Note is made for future reference that this theory includes the so-called finite-size scaling hypothesis that "close to the critical point, the microscopic length (lattice spacing) drops out."[9] A cautionary note has been mentioned by Brézin,[7] who says that finite-size scaling in this form holds only if "there is no singularity at the fixed point." He further points out that this hypothesis fails for spatial dimensions greater than or equal to 4 and "finite-size scaling does not hold there." One of the main accomplishments of this theory is the description of the phenomena of "finite-size rounding" of the peaks of thermodynamic functions such as the specific heat and the magnetic susceptibility. In the region of this rounding less general expressions are used, where the asymptotic form near the critical point of the divergent thermodynamic quantities, e.g., $\xi \propto (1 - K/K_c)^{-\nu}$, replaces the quantities themselves in at least part of the expressions. For example,

$$\begin{aligned} \chi(K, L) &= L^{\gamma/\nu} \phi_\chi((1 - K/K_c)\, L^{1/\nu}) \\ \xi(K, L) &= L \phi_\xi((1 - K/K_c)\, L^{1/\nu}) \end{aligned} \tag{4.4}$$

as $\chi \propto (1 - K/K_c)^{-\gamma}$, and for this model, $\nu = 1$, $\gamma = 7/4$. These equations can be combined to give

$$\chi = \xi^{\gamma/\nu} \frac{\phi_\chi((1 - K/K_c)\, L^{1/\nu})}{[\phi_\xi((1 - K/K_c)\, L^{1/\nu})]^{\gamma/\nu}} = \xi^{\gamma/\nu} \hat{\phi}((1 - K/K_c)\, L^{1/\nu}) \tag{4.5}$$

With this very brief sketch of some of the most elementary ideas of finite-size scaling, it seems worthwhile to look at how they might apply to good numbers for small systems. By means of the method described in the previous section, we have computed the energy, susceptibility, the second derivative of the susceptibility with respect to magnetic field, the correlation length, and the renormalized coupling constant for a series of temperatures. We have been able to carry out these calculations on the plane square lattice for square-shaped Ising models of sizes 2×2, 4×4, 6×6, 8×8, and 10×10. The last one corresponds to $2^{100} \approx 10^{30}$ states and was

carried out on an IPC sparc station. It required about 30 hr per temperature point in double precision. The only comparable computation that I know of is the computation of Bhanhot and Sastry[5] on the $4\times5\times5$ Ising model on the CM 2; however, they computed only the energy-type properties and neither the magnetic ones nor the correlation lengths. They pointed out that if one could generate one state every nanosecond, then it would take 4×10^{13} years to generate every state for a system this size. Our previous discussion suggests that form (2.30) should be asymptotically valid for small values of $|\mathbf{q}|$. We find this to be so for this model, where we can check the results against the high-temperature series results. The procedure we have used is to determine the correlation length by means of fitting (2.30) at the five points $\Delta k\,\mathbf{e}_x$, $\Delta k\,\mathbf{e}_y$, $2\,\Delta k\,\mathbf{e}_x$, $\Delta k(\mathbf{e}_x+\mathbf{e}_y)$, and $2\,\Delta k\,\mathbf{e}_y$, where the $\mathbf{e}_x$, $\mathbf{e}_y$ are unit vectors and Δk is the smallest value of $|\mathbf{q}|$ allowed by the lattice size and periodic boundary conditions. This fitting method was used, instead of just using two points, with an eye to the future use of these methods in Monte Carlo simulations for larger systems.

The value of the energy at the critical point is known to be $\sqrt{2}\approx1.4142136$. If we plot the values of the last line in Table I against $1/L$ we get a nice straight line. The linear projections from successive pairs are

$$1.434191,\quad 1.419372,\quad 1.415737,\quad 1.414858 \tag{4.6}$$

which is quite consistent with the limiting value, $\sqrt{2}$. This asymptotic form was given by Ferdinand and Fisher[12, 13] together with an evaluation of the coefficient of $1/L$. It is worthwhile to review at this point some of what is rigorously known. Ruelle[15] and Baker[1] showed that the limit $L\to\infty$ exists for the free energy per unit volume and is equal for free, periodic, and Dirichlet boundary conditions (see also Griffiths[18]). It has further been shown for the various multispin expectation values (since all are easily

Table I. Energy for the Plane Square Lattice

K/K_c	2×2	4×4	6×6	8×8	10×10
0.100	0.1771679	0.0885999	0.0884237	0.0884233	0.0884233
0.300	0.5489016	0.2783203	0.2724371	0.2723005	0.2722971
0.500	0.9428091	0.5199468	0.4826229	0.4793137	0.4789980
0.700	1.3099640	0.8863070	0.7724472	0.7425588	0.7347526
0.800	1.4642432	1.1227929	0.9892828	0.9320508	0.9076892
0.900	1.5933258	1.3618280	1.2587608	1.1991423	1.1613832
0.950	1.6482621	1.4699288	1.3945347	1.3507235	1.3213946
0.975	1.6734075	1.5194582	1.4579043	1.4236104	1.4013081
1.000	1.6970563	1.5656238	1.5168731	1.4915891	1.4762429

bounded from above for the Ising model) that a unique limit as $L \to \infty$ exists for Dirichlet boundary conditions. The energy is just twice the nearest-neighbor, spin–spin correlation. It is bounded from below for our case of periodic boundary conditions by the (monotonically increasing with system size) results for the Dirichlet boundary conditions. As it is the case[12] that the results for periodic boundary conditions for this model are monotonically decreasing, they, too, must tend to a unique limit. In this model we expect that the limits will be the same because the energy is continuous in the temperature in the usual thermodynamic limit at $T = T_c$ and so the rounding of the specific heat peak is not sufficient to show an effect in the infinite-system-size energy dependent on the model of approach to the limit or on the boundary conditions

If we plot (Fig. 6) the data in Table II in the form of $\xi_L(K)/L$ versus $\xi(K)/L$ we can see the data collapse implied by (4.2) beginning to emerge. We have used the simple approximation

$$\xi(K) = \left(\frac{K}{K_c}\right)^{1/2} \left(\frac{0.66384245 - 0.09664K/K_c}{1 - K/K_c}\right)$$

which is good enough for graphical purposes.

We might expect that [see (4.5)] $\hat{\phi}(x) \approx 2.597$, the value predicted by series analysis[2] and exact solutions[17] for an infinite system, since this quantity does not diverge, and both χ and ξ are derived from the same set of two-point correlation functions. If we use the data in the last lines of Tables II and III, we can compute the estimates for $\hat{\phi}(0)$ from the $2 \times 2, \ldots, 10 \times 10$ results,

$$\begin{gathered} 1.0128516, \quad 1.2689226, \quad 1.3921607 \\ 1.4509021, \quad 1.4837939 \end{gathered} \tag{4.7}$$

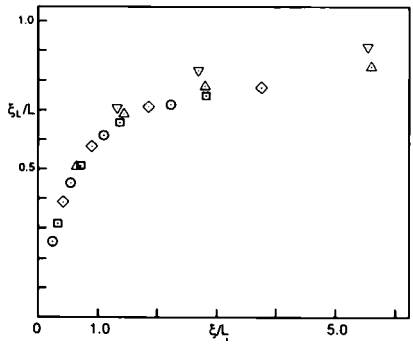

Fig. 6. A plot of ξ_L/L versus ξ/L. The 10×10 points are ⊙; the 8×8, ⊡; the 6×6, ◇; the 4×4, △; and the 2×2, ▽; using the data for $K/K_c = 0.8$, 0.9, 0.95, and 0.975.

Table II. Correlation Length Squared for the Plane Square Lattice

K/K_c	2×2	4×4	6×6	8×8	10×10
0.100	0.0528362	0.0530809	0.0530814	0.0530814	0.0530814
0.300	0.2349489	0.2489436	0.2492733	0.2492809	0.2492811
0.500	0.6035534	0.7493571	0.7647760	0.7661723	0.7663055
0.700	1.3496262	2.2885548	2.6433584	2.7488237	2.7776601
0.800	1.9729358	4.1107948	5.5213833	6.2777440	6.6365399
0.900	2.8597122	7.4223444	12.245941	16.674618	20.342144
0.950	3.4350623	9.9433196	18.296725	27.877511	37.972886
0.975	3.7630798	11.490710	22.295547	35.931821	51.844726
1.000	4.1213202	13.261699	27.078371	46.057374	70.243521

which appear to be converging. If we plot these values against $1/L$, they form a downward-curving plot, from $L=4$ onward. Thus the limit would appear to be less than 1.615, the last linear extrapolation. Analysis of other data in those tables is not inconsistent with $\hat{\phi}(\infty)=2.597$, which relates to the thermodynamic properties, but the data are insufficiently extensive to be more definite on this point. It is, however, reasonably clear that $\hat{\phi}$ is not a constant. In this case, in contrast to the energy, the method of approach to the limit does matter. Since the limit for the nearest-neighbor spin–spin correlations is unique, it is reasonable to suppose that the limit for all the $\langle\sigma_0\sigma_{\mathbf{i}}\rangle$ are unique for fixed $\mathbf{i}$ and the rounding effects come from the behavior where the limit of $|\mathbf{i}|/L\neq0$. (See also Binder.[6])

An additional thing to check, where the descrepancy is perhaps clearer, is comparison of the data in Tables III and IV. Here, since $\partial^2\chi/\partial H^2 \propto (1-K/K_c)^{-\gamma-2\Delta}$, we expect, as $(\gamma+2\Delta)/\gamma=22/7$, that

$$\mathscr{R}=-\frac{\partial^2\chi/\partial H^2}{\chi^{22/7}}=\bar{\phi}\left(\left(1-\frac{K}{K_c}\right)L^{1/\nu}\right) \tag{4.8}$$

Table III. Susceptibility for the Plane Square Lattice

K/K_c	2×2	4×4	6×6	8×8	10×10
0.100	1.1926232	1.2029176	1.2029381	1.2029382	1.2029382
0.300	1.6818679	1.8571952	1.8612700	1.8613647	1.8613671
0.500	2.2761424	3.2174771	3.3207033	3.3301475	3.3310512
0.700	2.8625812	6.0806596	7.4708853	7.9018527	8.0218031
0.800	3.1140275	8.1550547	12.030997	14.277760	15.394867
0.900	3.3259424	10.319413	18.500643	26.499145	33.541128
0.950	3.4164830	11.307150	21.892778	34.173759	47.404871
0.975	3.4579876	11.759990	23.482752	37.917550	54.554732
1.000	3.4970563	12.181742	24.959397	41.402340	61.256766

Table IV. Values of $-\partial^2\chi/\partial H^2$ for the Plane Square Lattice

K/K_c	2×2	4×4	6×6	8×8	10×10
0.100	3.8934981	4.0994029	4.1001545	4.1001567	4.1001567
0.300	12.236472	19.790775	20.142356	20.154205	20.154591
0.500	29.751612	121.11544	146.22125	149.70451	150.13863
0.700	55.215452	763.51622	1820.7032	2445.1974	2696.5710
0.800	68.642864	1644.8706	6783.0126	13713.541	19560.869
0.900	81.131933	2953.1381	20225.894	69246.927	160961.74
0.950	86.795217	3682.3435	30361.803	128586.25	377428.45
0.975	89.456859	4044.0651	35839.108	164421.32	526633.92
1.000	91.999930	4396.2815	41334.453	201763.97	689322.40

where again we might expect that $\bar{\phi}(x) = 4.93$ as predicted by series analysis and exact solutions, in the absence of different, finite-size roundings. If we use the data in the last lines of Tables III and IV, we can compute the estimates for $\bar{\phi}(0)$ from the $2\times2,\ldots,10\times10$ results,

$$1.7989033,\quad 1.7015941,\quad 1.6788236$$
$$1.6701881,\quad 1.6659136 \tag{4.9}$$

which appear to be converging to a value less than 1.666. In this case, the values of $\mathscr{R}$ begin at 2 for $K=0$, rise to a peak, and then fall back to the values in (4.9) as $K\to K_c$. The height of the peak is steadly increasing as L increases, but has not yet reached the expected value at 4.93. Again the numerical results are not inconsistent with expectations.

One quantity of considerable interest is the renormalized coupling constant g^*. In the field theory implementation of the renormalization group theory of critical phenomena, it is this quantity which is the key parameter of the theory and is universal for models within the basin of attraction of the renormalization-group fixed point. If it is nonzero (it can be proven to be both nonnegative and finite), then the theory predicts that the hyperscaling relations between the various critical indices hold. These are the critical index equalities which depend explicitly on the spatial dimension. If $g^*=0$, as is true for spatial dimension greater than or equal to 4, then those relations may no longer be valid. The definition is

$$g(K) = -\frac{v}{a^d}\frac{\partial^2\chi(K)/\partial H^2}{\chi^2(K)\,\xi^d(K)}$$
$$g^* = \lim_{K\to K_c^-} g(K) \tag{4.10}$$

where a is the lattice spacing, v is the volume per lattice site, and d is the spatial dimension. The value for the $d=2$ Ising models on both the plane square and the triangular lattices is estimated to be 14.66 ± 0.06 by series methods.[2] The results of our computations for the renormalized coupling constant are given in Table V. If we plot $g(K_c)$ against $1/\sqrt{L}$, we get a curve with a small negative curvature for $L \geqslant 4$. The last two points give a linear extrapolation of about 3.12; thus it would appear that the infinite-size limit is no greater than this value and so is much smaller than the 14.66 quoted above. This point is apparently a point of nonuniform approach in K and L as will be further discussed below. Since for two dimensions $g(K) \propto 1/K$ for small K, it is more convenient to dipslay these results in the form of $Kg(K)/K_c$ versus K/K_c as shown in Fig. 7. By a comparison of these results with the series solution for $g(K)$ for an infinite system and our results for $\xi_L(K)$ we see that the finite-size results are an accurate reflection of the infinite limit within about 1% or so, so long as $\xi/L \leqslant 1/(7 \pm 1)$. This restriction is more severe than is often used in practice, and the corresponding $\Phi_g(x)$, (4.2), is, of course, fairly closely x in this region. The error increases quite rapidly beyond this point and the evaluation of g becomes quite significantly inaccurate for values of the ratio only modestly larger and the use of such a larger ratio can lead to results with large errors due to the strong rounding effects.

It is of interest to note that the quantity g^*_- for which the limit in (4.10) is taken for $K > K_c$ instead of as indicated therein has quite a different value. To compute it, we use the series analysis values of Essam and Hunter,[11] plus the exact value (instead of the spherical moment definition which we use elsewhere) for $\xi_-(K) = 1/[8(K-K_c)]$. The result is $g^*_- \approx -656$. The main reasons that this value is so different from that on the other side are that $\partial^2\chi/\partial H^2$ changes sign and the amplitude for χ_- is

Table V. Values of $g(K)$ for the Plane Square Lattice

K/K_c	2×2	4×4	6×6	8×8	10×10
0.100	51.808555	53.371676	53.379140	53.379164	53.379164
0.300	18.411918	23.048720	23.324685	23.335320	23.335690
0.500	9.5147184	15.612763	17.338683	17.619010	17.657446
0.700	4.9926543	9.0230958	12.340676	14.246532	15.086509
0.800	3.5878770	6.0166146	8.4873375	10.715831	12.436396
0.900	2.5647206	3.7362217	4.8254954	5.9139940	7.0334853
0.950	2.1647246	2.8965870	3.4622024	3.9496174	4.4229810
0.975	1.9880319	2.5448217	2.9150168	3.1827194	3.4130244
1.000	1.8253489	2.2339195	2.4503126	2.5556106	2.6152185

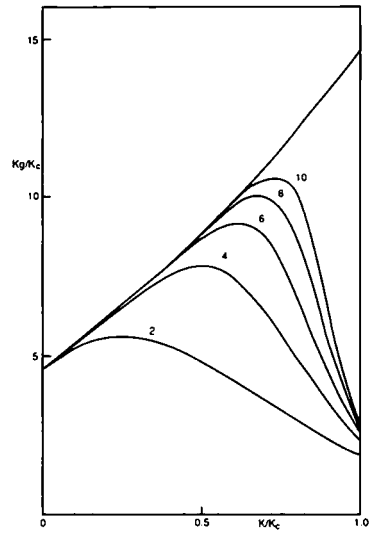

Fig. 7. A plot of $Kg(K)/K_c$ versus K/K_c. The curves are labeled according to system size. The unlabled curve is the series result for an infinite system.

only 0.02568 instead of 0.9624 for χ_+. In this context, we see that the "rounded value" of g^* computed at $K = K_c$ is intermediate between that for g_+^* and g_-^*. This situation is in contrast to that for the energy, which as we have pointed out has no rounding and is continuous at $K = K_c$. The effect of the rounding on g^* is really quite different from that on quantities which are usually discussed. For example, the specific heat is rounded, but nevertheless the value computed as the system size goes to infinity for $K = K_c$ is infinity, which is the correct thermodynamic value. But, to reiterate, the same is not true of g^*, since the critical point is a point of nonuniform approach and different values are obtained, depending on the direction of approach. The same effect is expected in the three-dimensional Ising model[11] because $\partial^2\chi/\partial H^2$ also changes sign and is discontinuous at the critical point in that model.

It is also of interest to consider Binder's cumulant ratio.[6] It is closely related to $g(K)$ and is defined for $K \leqslant K_c$ by

$$U_L = -\frac{\partial^2\chi(K)/\partial H^2}{3L^d\chi^2(K)} \tag{4.11}$$

for a system of size L at inverse temperature K. Binder argued from finite-size scaling theory that U_L is a universal function of ξ/L. For $K < K_c$, the theory indicates that it goes to zero as $L \to \infty$, while for $K > K_c$ it goes to

2/3. Exactly at $K = K_c$ it goes to a fixed point value U^*. From the data in Tables III and IV, we find, as a function of L for $K = K_c$, that

$$U_L = 0.62690394, \quad 0.61719935, \quad 0.61435622, \quad 0.61304536, \quad 0.61234053 \tag{4.12}$$

while for $K/K_c = 0.975$,

$$U_L = 0.62342690, \quad 0.60920435, \quad 0.60177682, \quad 0.59562973, \quad 0.58982438 \tag{4.13}$$

The values for $K = K_c$ agree with those given by Burkhardt and Derrida[8] to the accuracy that they quote. The recommended way to locate the critical point by this method is to look at the crossing of U_L and $U_{L'}$ for $L \neq L'$. Because of the structure of these functions, they should be equal and have different slopes at the critical point. We find by linear extrapolation that U_8 and U_{10} cross at $K_{c,8,10}/K_c \approx 1.00345$, which is an order of magnitude more accurate than the peak location for the specific heat,[12] which is at about $K_{\text{peak}}/K_c \approx 0.965$.

A key problem for people who attempt to deduce the behavior of the thermodynamic limit from the behavior of finite-size systems is how to extrapolate to the infinite limit. It is worthwhile to consider the different cases that can arrise. For small values of K, we consider the series expansion in K, for example, for the susceptibility. The difference between the finite system with periodic boundary conditions and the infinite system first appears in the Lth order. The graphs which represent the susceptibility are certain connected graphs which have just two odd vertices. In Lth order, the L-edged, straight-line graphs of the infinite system instead overlap their beginning and end points and form L-edged polygons with no odd vertices. This change gives a correction from the infinite system to the finite one of $-4K^L$ as the leading-order correction. Hence the error for small K is basically exponentially decaying with system size. At the critical point, as we have seen above from finite-size scaling theory, the behavior is best thought of for χ^{-1}, which has the value zero at the critical temperature. Here the error is given by $1/[\Phi_\chi(0)\, L^{\gamma/\nu}]$ and is a power law. For the intermediate values of K, these results suggest that the error may again decay exponentially asymptotically, but manifests this behavior only for increasingly large system size with an intermediate region of power-law decay. As we say, for $K = K_c$, the error in the energy decays like $1/L$, but for ratios of divergent quantities, for example, g, the effects of rounding are such that the limit as $L \to \infty$ for $K = K_c$ gives a rounded answer which is different from the thermodynamic answer. In these cases a double limit is in principle necessary,

where we first estimate the behavior as $L \to \infty$ and then the limit as $K \to K_c$. For a predetermined level of accuracy, this double limit can be replaced by a single limit with $K \to K_c$ and $L \to \infty$ together. The physical argument is that the correct thermodynamic limit is obtained by "finite-size scaling" for values of $\xi_L(K)/L$ sufficiently small and thus the limit is taken for $L \to \infty$ with ξ/L held fixed. Some investigation of what "sufficiently small" means must be carried out by considering various cases where $\xi_L(K)$ is big compared to unity and small compared to L.

REFERENCES

1. G. A. Baker, Jr., *J. Math. Phys.* **16**:1324 (1975).
2. G. A. Baker, Jr., *Phys. Rev. B* **15**:1552 (1977).
3. G. A. Baker, Jr., *J. Stat. Phys.* **72**:621 (1993).
4. M. N. Barber, in *Phase Transitions and Critical Phenomena*, Vol. 8, C. Domb and J. L. Lebowitz, eds. (Academic Press, London, 1983), p. 145.
5. G. Bhanot and S. Sastry, *J. Stat. Phys.* **60**:333 (1990).
6. K. Binder, *Z. Phys. B* **43**:119 (1981).
7. E. Brézin, *J. Phys.* (Paris) **43**:15 (1982).
8. T. W. Burkhardt and B. Derrida, *Phys. Rev. B* **32**:7273 (1985).
9. J. L. Cardy, ed., *Finite-Size Scaling* (North Holland, Amsterdam, 1988).
10. F. Cooper, B. Freedman, and D. Preston, *Nucl. Phys. B* **210**[FS6]:210 (1982).
11. J. W. Essam and D. L. Hunter, *J. Phys. C* **1**:392 (1968).
12. A. E. Ferdinand, Lattice statistics of finite systems, Thesis, Cornell University (1967).
13. A. E. Ferdinand and M. E. Fisher, *Phys. Rev.* **185**:832 (1969).
14. V. Privman, *Finite Size Scaling and Numerical Simulation of Statistical Systems* (World Scientific, Singapore, 1990).
15. D. Ruelle, *Statistical Mechanics* (Benjamin, New York, 1969).
16. M. F. Sykes, J. W. Essam, B. R. Heap, and B. J. Hiley, *J. Math. Phys.* **7**:1557 (1966).
17. C. A. Tracy and B. M. McCoy, *Phys. Rev. Lett.* **31**:1500 (1973).
18. R. B. Griffiths, *J. Math. Phys.* **8**:484 (1967).